Fiber dispersion in the corpus callosum revealed with postmortem diffusion weighted imaging and PLI

Submission Number:

6248

Submission Type:

Abstract Submission

Authors:

Jeroen Mollink[1], Michiel Kleinnijenhuis[1], Saad Jbabdi[1], Stamatios Sotiropoulos[1], Olaf Ansorge[2], Karla Miller[1]

Institutions:

[1]FMRIB centre, University of Oxford, Oxford, United Kingdom, [2]Department of Clinical Neurology, University of Oxford, Oxford, United Kingdom

Introduction:

Diffusion weighted imaging infers the microstructural architecture of brain tissue by detecting alterations to diffusive motion along different orientations. Increasingly sophisticated models are used to describe the underlying biophysical mechanisms of diffusivity. In this respect, the human corpus callosum (CC) often functions as a test-bed for such biophysical models (Nilsson, 2013), because of its assumed pronounced fiber coherence. However, this hypothesis might not always be appropriate as recent work demonstrated a considerable amount of dispersion in the CC (Budde, 2013; Mikula, 2012; Leergaard, 2010). Here, we aim to replicate those findings with postmortem diffusion weighted imaging applied to the ball and racket model (Sotiropoulos, 2012) and additional diffusion time STEAM measurements. We expect the latter to be particularly sensitive to deviation of tracts from the common assumption of straight, parallel cylinders, as evidence for hindrance along tracts was previously found with in vivo STEAM experiments in the CC (Lam, 2015). Additionally, polarized light imaging (PLI), was applied to the same specimen to confirm dispersion measures from the ball and racket model. PLI is a microscopy technique that allows for quantification of myelin orientation based on its optical birefringence.

Methods:

A 5 mm coronal slab was excised from a fixed brain at the level of the anterior commissure, including the CC and the gyri cinguli. It was scanned on a 9.4 T Varian MRI scanner. STEAM diffusion (DW-STEAM) data were acquired with diffusion gradients (δ=2.22 ms) applied in 30 directions distributed over a hemisphere for 9 diffusion times Δ = [35 70 100 150 200 250 300 350 400] ms with a fixed q-value (0.14 rad/μm). For each diffusion time, a non-diffusion weighted image was acquired. Imaging parameters: 10 slices with 0.4 mm isotropic voxels, TE=16ms, TR=2.4-4.1 s. Spin echo diffusion (DW-SE) data were acquired with TR/TE=2.4s/29ms, 240 directions (δ=6ms, Δ=16ms) with b=[2500,5000] s*mm^-2. To estimate within-voxel orientation dispersion from the DW-SE data, the ball and racket model was fitted. Following MRI, the same sample was frozen and cut in 60 μm sections. PLI was performed with a polarizing microscope and fiber orientation maps were computed as described previously (Axer, 2011). In-plane fiber dispersion was estimated by fitting the fiber orientation distribution with a von Mises distribution for a certain neighbourhood. The concentration parameter (κ) of the von Mises was correlated with 95% angular difference of the mean angle of the fiber orientation distribution. Results were analyzed for the middle and lateral CC seperately (Fig 3).

Results:

The DW-SE data and PLI demonstrate great correspondence of the macroscopic primary fiber orientation after qualitative inspection of both fiber orientation maps (Fig. 1). Dispersion as computed by the ball and racket model shows higher dispersion in middle part than at lateral regions of the CC. Though PLI also demonstrated dispersion in the CC (Fig 3), the patterns of both dispersion maps did not match exactly, i.e especially the right portion of the CC had higher dispersion than was estimated with the ball and racket model (Fig 2). It should be noted that this is only a qualitative comparison as both modalities house a different measure for fiber dispersion. For the very long diffusion times employed with DW-STEAM, ADC behaves as if hindered both across and along the axonal orientation i.e. ADC decreases with diffusion time.

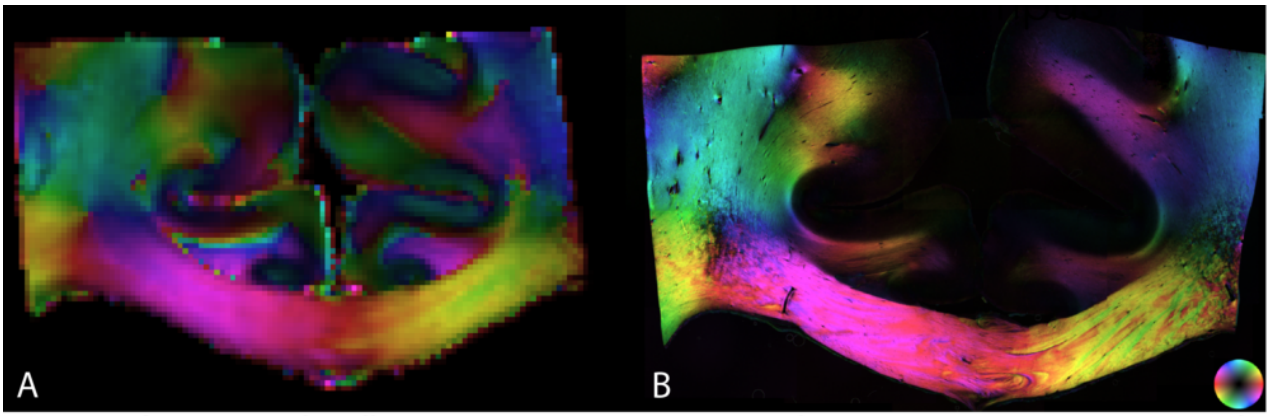

Figure 1. HSV colormap for diffusion MRI (A) and PLI (B) in-plane fiber orientation. Hue channel codes for the angular orientation, the saturation channel is constant and the value channel codes for either FA or the birefringence in diffusion MRI and PLI, respectively.

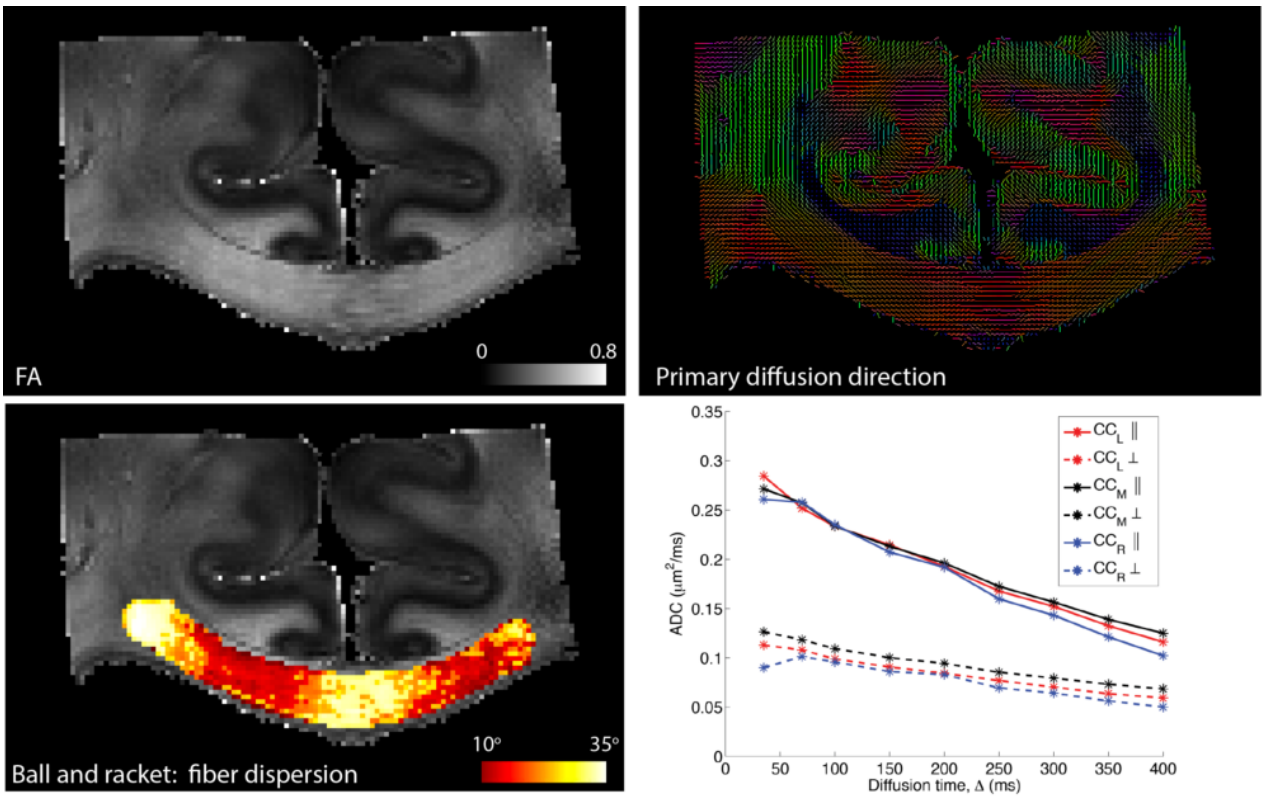

Figure 2: Diffusion weighted imaging data for SE and STEAM sequences. Top figures indicate FA and primary diffusion direction maps for the DW-SE data. Within voxel-dispersion was estimated with the ball and racket fanning model. Middle part of the corpus callosum exhibited higher fiber orientation dispersion as compared to lateral sides. Even more lateral near the left centrum semiovale, fiber dispersion is high due to crossing fibers in this region. The graph depicts the apparent diffusion coefficients (ADC) from STEAM data at different diffusion times for diffusion parallel and perpendicular to the fiber orientation in the corpus callosum regions. Interestingly, parallel to the axons, hindered diffusion is observed as diffusion time extends.

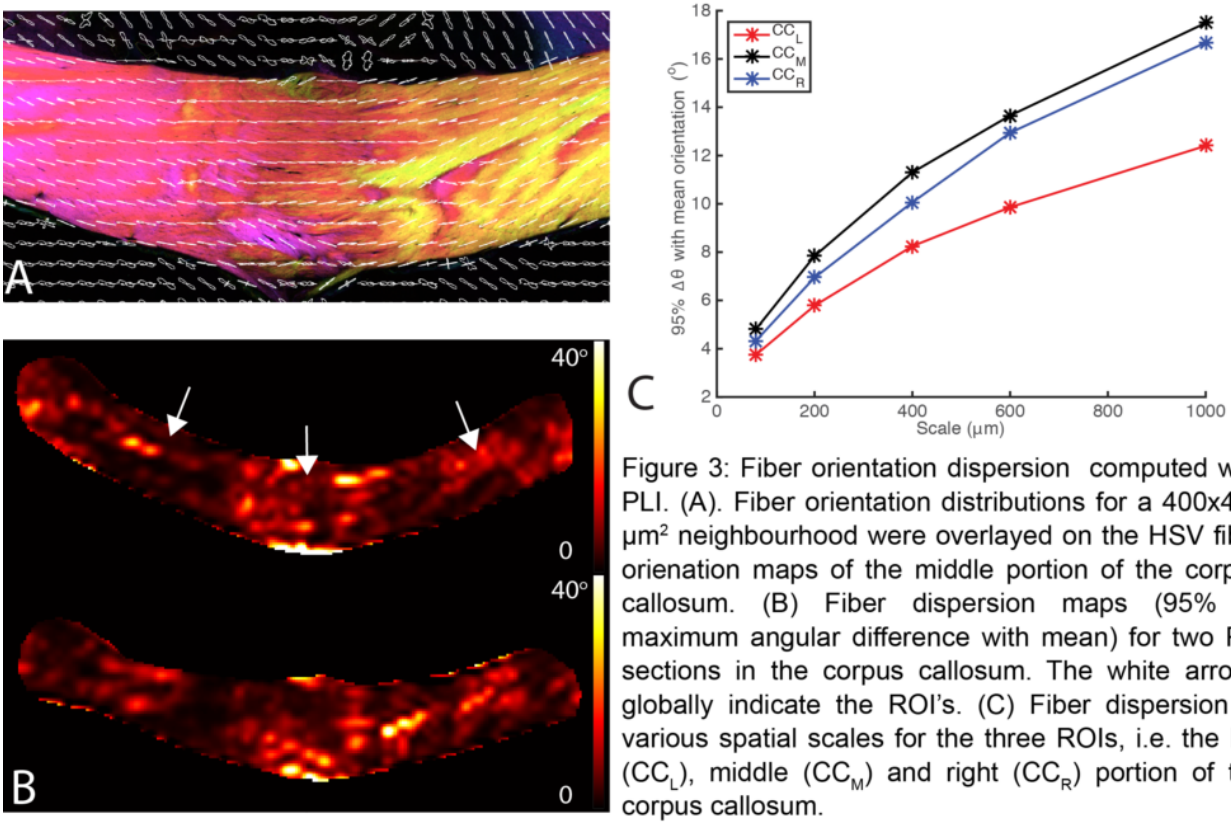

Figure 3: Fiber orientation dispersion computed with PLI. (A). Fiber orientation distributions for a 400x400 μm² neighbourhood were overlayed on the HSV fiber orienation maps of the middle portion of the corpus callosum. (B) Fiber dispersion maps (95% of maximum angular difference with mean) for two PLI sections in the corpus callosum. The white arrows globally indicate the ROI's. (C) Fiber dispersion at various spatial scales for the three ROIs, i.e. the left (CC_L), middle (CC_M) and right (CC_R) portion of the corpus callosum.

Conclusions:

The results demonstrated here support our hypothesis that the CC is not as coherent as often is assumed. Diffusion imaging employing long diffusion times might provide better understanding in the behaviour of water molecules within fiber bundles, though more sophisticated analysis methods are desirable. The inclusion of diffusion simulations in existing fiber geometries would be an essential tool to complement such studies.

Imaging Methods:

Polarized light imaging (PLI) [2]

Modeling and Analysis Methods:

Diffusion MRI Modeling and Analysis

Neuroanatomy:

White Matter Anatomy, Fiber Pathways and Connectivity [1]

Keywords:

MRI

Myelin

OPTICAL

White Matter

[1]|[2]Indicates the priority used for review

Would you accept an oral presentation if your abstract is selected for an oral session?

Yes

Please indicate below if your study was a "resting state" or "task-activation" study.

Other

Healthy subjects only or patients (note that patient studies may also involve healthy subjects):

Healthy subjects

Internal Review Board (IRB) or Animal Use and Care Committee (AUCC) Approval. Please indicate approval below. Please note: Failure to have IRB or AUCC approval, if applicable will lead to automatic rejection of abstract.

Not applicable

Please indicate which methods were used in your research:

Structural MRI

Optical Imaging

Diffusion MRI

Postmortem anatomy

Which processing packages did you use for your study?

FSL

Provide references in author date format

Axer, M. (2011). High-resolution fiber tract reconstruction in the human brain by means of three-dimensional polarized light imaging. Frontiers in neuroinformatics, 5, p.34.
Budde, M.D. (2013). Quantification of anisotropy and fiber orientation in human brain histological sections. Frontiers in integrative neuroscience, 7, p.3.
Lam, W.W. 2015, 'Quantification of Microscopic Brain Structures Using Diffusion Magnetic Resonance', PhD thesis, 2015.
Leergaard, T.B. (2010). Quantitative histological validation of diffusion MRI fiber orientation distributions in the rat brain. P. A. Valdes-Sosa, ed. PloS one, 5(1), p.e8595.
Mikula, S (2012). Staining and embedding the whole mouse brain for electron microscopy. Nature methods, 9(12), pp.1198–201.
Nilsson, M (2013). The role of tissue microstructure and water exchange in biophysical modelling of diffusion in white matter. Magma, 26(4), 345–70.
Sotiropoulos, SN (2012). Ball and rackets: Inferring fiber fanning from diffusion-weighted MRI. Neuroimage. 60(2):1412-25